This is a non-peer reviewed pre-print submitted to EarthArXiV.

This manuscript has undergone peer-review for Journal of Glaciology. It was accepted with revisions; however, the corrected version has not been resubmitted. If further proceeded, the final version of this manuscript may have slightly different content.

The author welcome feedback.

Please contact Aleksandra K. Mazur (akmazur@gmail.com) regarding this manuscript's content.

Seasonal changes of iceberg distribution and surface area in the Amundsen Sea Embayment

A. K. Mazur[a,b]*, A. K. Wåhlin[a] and S. Swart[a,c]

[a]*Department of Marine Sciences, University of Gothenburg, Göteborg, Sweden;* [b]*Institute of Oceanography, University of Gdańsk, Gdynia, Poland;* [c]*Department of Oceanography, University of Cape Town, Rondebosch, South Africa.*

*corresponding author: A. K. Mazur, Department of Marine Sciences, University of Gothenburg, PO Box 461, 405 30 Göteborg, Sweden, e-mail: akmazur@gmail.com

ABSTRACT

Icebergs have a significant influence on local and potentially global climate by altering ocean and sea ice environments. An object-based method for automatic iceberg detection has been applied to 2442 SAR images acquired during all seasons between 2006-2012 in the Amundsen Sea Embayment (ASE), Antarctica. During this period a total count of icebergs and their surface area were calculated in different seasons and months. There is a clear seasonal variability in icebergs number and surface area in the ASE. The highest values of both parameters are observed during austral winter, the lowest during austral summer. The changes concern mostly the icebergs smaller than 2 km^2 and pertain to the area north of the Pine Island Bay. A general westward drift of icebergs was observed in the ASE shelf area. The drift patterns and the seasonal variation of the distribution indicate that the drift of icebergs in the northern part of the ASE is strongly modulated by sea ice. They indicate mostly allochtonous origin of those bergs (icebergs imported from the Bellingshausen Sea represent about 25-35% of the total surface

area of mobile icebergs in the Amundsen Sea). This is a new result not previously studied in the literature.

Keywords: icebergs, the Amundsen Sea, satellite radar data, object-based image analysis, iceberg seasonal and monthly distribution changes, iceberg drift

1. INTRODUCTION

Icebergs are pieces of freshwater ice that can be either freely drifting or grounded on submerged ridges or shallow banks. Grounded icebergs can significantly influence the local water circulation, e.g., they serve as a barrier for sea ice drift, fosters sea ice opening on the lee side (Hunke and Ackley, 2001) or drive a local upwelling analogous to wind-driven coastal upwelling (Stern and others, 2015) but most of all icebergs can weaken and delay the effect of global warming in the Southern Hemisphere (Schloesser and others, 2019). During their drift, icebergs decay and melt contributing to freshwater content in the water column (e.g., Biddle and others, 2015). They also have an impact on primary production (e.g., Raiswell and others, 2008; Lancelot and others, 2009), which is thought to be stimulated by the release of iron-rich terrigenous material in the vicinity of icebergs (e.g., Smith and others, 2007). Drifting icebergs can also pose a threat to benthic organisms (Barnes, 2017). Increasing mortality of the encrusting benthos may lead to decreasing the amount of immobilized carbon stocks and its recycling.

The West Antarctic Ice Sheet (WAIS) alone contains such an amount of ice that if the whole volume melted the global sea level would rise by about 3.3 – 4.3m (Bamber and others, 2009, Fretwell and others, 2013). Glaciers that drain into the Amundsen Sea Embayment (ASE) are currently contributing the most towards sea level rise. It is estimated that about 50% (670 Gt yr^{-1}) of the Antarctic ice loss is from ice shelves in the ASE and iceberg calving amounts of almost 30% of the total value (Depoorter and others, 2013, Rignot and others, 2013). Large quantities of glacial melt water have been observed in the water column on the ASE shelf (e.g., Wåhlin and others, 2010, Arneborg and others, 2012, Jacobs and others, 2012) (Fig. 1). However, it is not yet clear how much of the observed meltwater originates in glaciers and how much comes from icebergs already detached from the glaciers (Wåhlin and others, 2010).

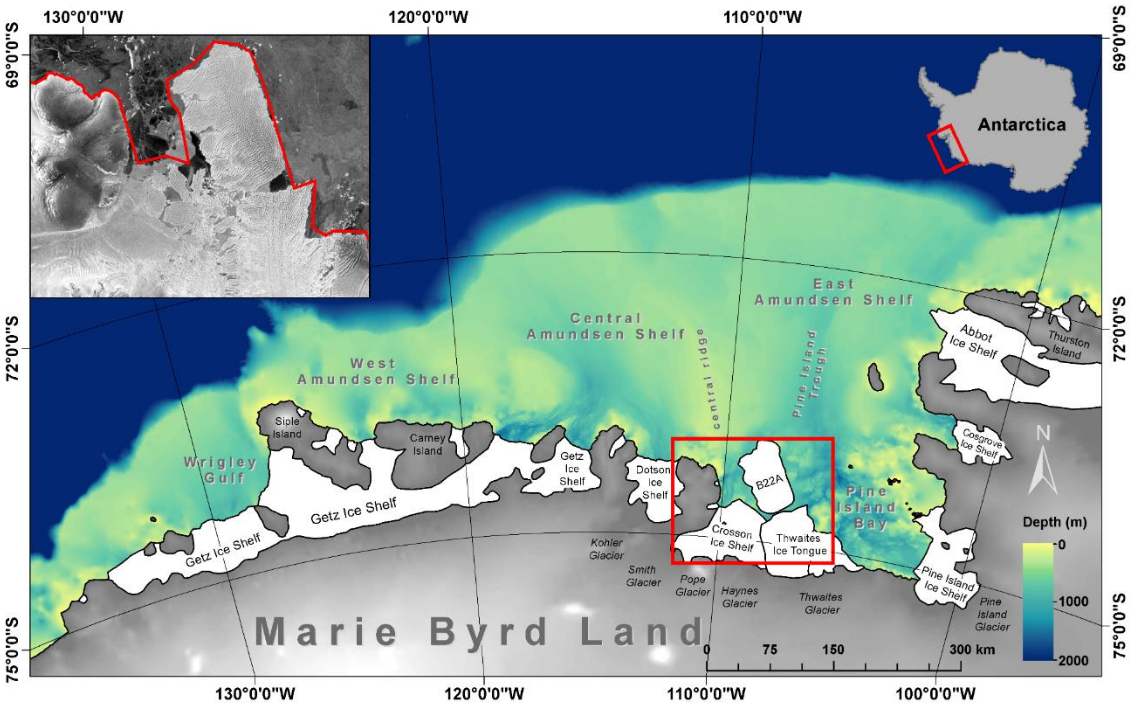

Figure 1. Location and bathymetry of the ASE. The bathymetry is acquired from International Bathymetric Chart of the Southern Ocean (IBCSO) database (Arndt and others, 2013). A radar image showing the area excluded from the present analysis is presented in upper left corner.

There is number of modelling studies of iceberg meltwater presence and distribution in the Southern Ocean. Gladstone and others (2001) and Merino and others (2016) in their estimations of meltwater injection focused on small icebergs (not longer than 3 km) and assumed constant in time iceberg release from individual source locations. Silva and others (2006) complemented their model with available observation of giant icebergs, whereas Rackow and others (2017) initialized their model with a set of observed iceberg positions (of all sizes) around Antarctica. They were icebergs detected by Wesche and Dierking (2015) in September/October 1997. Gladstone and others (2001) in their model observed no clear seasonal trends of iceberg movement patterns and thus assumed that even if seasonality in iceberg calving may exist it would not have a large effect on iceberg meltwater distribution. An opposing view by Merino and others (2016) show strong seasonality of freshwater flux (with the highest values observed in January and February), which is particularly seen in the Amundsen and Ross Seas and they estimated an average iceberg freshwater flux of around 25 Gt in the Pacific sector of the Southern Ocean. Silva and others (2006) demonstrated that giant icebergs have to be taken into account while modeling iceberg meltwater distribution as their spatial distribution and temporal variability differ significantly from smaller icebergs. Is it also confirmed in the study of Rackow and others (2017) who noted that seasonality of freshwater input successively decreases when larger icebergs are included into the model.

According to Mazur and others (2019) icebergs smaller than 2 km^2 contribute to the majority of the total iceberg number variability in the ASE. This is important because it can be expected that the melting from small icebergs is more efficient than melting of the large ones due to the ratio between surface area of contact with sea water is much larger. This suggests the distribution of smaller bergs has a larger impact on freshwater fluxes to the surface ocean. Additionally, the small icebergs (smaller than 2 km^2) can be found all over the ASE, with slightly higher probability in the area north of Pine Island Bay (Mazur and others, 2019) but there is little known about seasonal changes in their distribution. The main motivation for the present study was to study how iceberg characteristics, such as their number, surface area and spatial distribution changes in different seasons and months. The main scientific question is if there is a seasonal variation in iceberg number and their spatial distribution. This information can be important in order to better validate existing models.

Recently Mazur and others (2017) presented an object-based method of iceberg identification and classification from Envisat Advanced Synthetic Aperture Radar Wide Swath Mode (ASAR WSM) images. The classification results tend to be similar regardless of the season, also it performs well for small icebergs (smaller than 2 km^2), prevailing in the ASE. In this work the technique presented by Mazur and others (2017) was applied to Envisat ASAR WSM images acquired between 1 January 2006 and 8 April 2012.

The paper describes seasonal estimates of the number, surface area of icebergs and their drift patterns in connection to the ocean surface stress (Kim and others, 2017). To our knowledge it is the first study where seasonal iceberg characteristics in the ASE were studied based on satellite observations.

2. DATA

2.1. Satellite radar data

Synthetic Aperture Radar (SAR) data are high-resolution images of the Earth surface that can be obtained regardless of daylight and cloudiness. In this study Envisat ASAR WSM data were used. They were 2445 Level 1b images recorded between 1 January 2006 and 8 April 2012. The images were acquired at C-band (5.3 GHz) and HH polarization using the ScanSAR technique at spatial resolution 150 m × 150 m and the incidence angle varied between 17° – 43° (Envisat ASAR Product Handbook, 2007).

2.2. Sea ice concentration data

The sea ice concentration data used here were daily 6.25 km × 6.25 km resolution products provided by University of Bremen between 1 January 2006 and 8 April 2012 (https://seaice.uni-bremen.de). The sea ice concentration was acquired from Advanced Microwave Scanning Radiometer–Earth Observing System (AMSR–E) (Spreen and others, 2008) and Special Sensor Microwave Imager/Sounder (SSMIS) after AMSR-E stopped working on 04 October 2011. The SSMIS based maps have lower resolution, but for compatibility reasons University of Bremen provides them at the same grid spacing as the AMSR–E products.

2.3. Ocean Surface Stress

The ocean surface stress data used in this study were provided by Kim and others (2017). The term ‘ocean stress’ is used to describe how the presence of sea ice may affect this momentum exchange, taking into account the momentum transfers from either (or both) air-ocean stress and ice-ocean stress. The ocean surface stress was calculated by a combination of the ice – ocean and the air – ocean surface stress. In regions with 100% ice coverage, the ice – ocean surface stress based on the ice drift velocity was applied. In ice-free regions, the direct wind stress was applied. In regions with partial ice coverage the surface stress was calculated by combining the two weighting by the ice concentration (Kim and others, 2017). In the present study monthly averages of the stress calculated on a 1° × 1° grid between 1 January 2010 and 31 December 2011 were used.

3. METHODS

3.1. Iceberg calving estimation

Iceberg calving into the embayment was estimated in accordance with the method described by Liu and others (2015) and Mazur and others (2019). As the ice front is advancing and the ice shelf position moves during the year the images were first aligned using feature tracking. The calved area was then calculated by digitizing the difference between the aligned images. The analyzed images (4-5 per month to cover the whole ASE) were acquired at the beginning of each month between 1 January 2011 and 31 December 2012.

In this study, ice mass loss is calculated from the actual area loss every month multiplied by the mean ice equivalent thickness at the shelf front and the ice density. Since the actual ice thickness of ice shelves is a combination of marine ice and a firn layer (an intermediate stage between snow and glacial ice) that have different densities, here we use the ice equivalent thickness presented by Liu and others (2015). The ice equivalent thickness is the thickness the ice shelf would have assuming an average ice density 917 kg m^{-3}.

3.2. Iceberg classification

To detect and classify icebergs we used the method described in Mazur and others (2017) and applied it to ASAR images acquired between 1 January 2006 and 31 December 2012 to construct a time series of iceberg presence and area. The classification algorithm presented by Mazur and others (2017) is based on an object-oriented image interpretation with segmentation and classification carried out on different scale levels. Icebergs are separated from the background, which can be either open water or sea ice, based on brightness, contrast and shape qualities with thresholds given on each scale.

The average detection rate of the algorithm was 96.2%, which corresponded to 93.2% of the iceberg area. The rate of errors in the form of 'false alarms' and 'misses' was 3.9% and 3.8%, respectively (Mazur and others, 2017). However, the values differed depending on the season. False alarms appear mostly in areas where wind-roughened open water or highly deformed sea ice floes are present, which is observed particularly in austral spring and autumn. The backscatter coefficient of such sea ice floes or wind-roughened water overlaps with that of icebergs, and they also tend to form quite compact objects with high contrast to the surrounding water. The detection rate, and the rate of 'false alarms' and 'misses' for individual seasons are presented in Table 1.

Table 1. The detection rate, and the rate of 'false alarms' and 'misses' in different seasons, calculated based on iceberg number and their surface area.

	Summer		Autumn		Winter		Spring	
	Numbe	Area	Number	Area	Number	Area	Numbe	Area
Detection rate	93.8	91.6	95.6	93.8	97.9	92.8	98.0	96.7
Misses (%)	6.2	8.4	4.4	6.2	2.1	7.2	2.0	3.3
False alarms (%)	3.3	7.5	3.7	13.8	4.5	13.1	3.6	16.0

As the ASAR images were captured somewhat irregularly in space and time, certain regions have much better coverage than others and the coverage varies in time. For this reason, the number of icebergs and their surface area are presented in relation to the coverage in a gridded field (15 km × 15 km) as basis. Total iceberg number and surface area were obtained by adding up all the average values for the grid cells.

The study area here was the ASE which was determined by 2000 m isobaths and no data falls outside of this domain. Also similarly to Mazur and others (2019), the area at the mouth of the Crosson Ice Shelf and Thwaites Ice Tongue (Fig. 1, upper left subset) has a large number of grounded bergs surrounded by a mixture of small, clustered bergs frozen within sea ice, only unreliably detectable with the available imagery resolution. This area, plus the area occupied by iceberg B22A (approximately 3500 km^2 in size and considered as a separate ice island), was excluded from the present analysis. Only icebergs leaving these regions were counted.

4. RESULTS

4.1. Seasonal changes of iceberg characteristics

The total average number and surface area of icebergs were calculated in different seasons: summer (December – February), autumn (March – May), winter (June – August), spring (September – November) and presented in Fig. 2. Between 2006 – 2009 the Envisat satellite was not focused on acquisition of the data over the ASE and there was incomplete data coverage during certain seasons (marked with asterisks in Fig. 2). That could lead to somewhat an underestimate or overestimate in number and surface area of icebergs. However, as the regions with lack of the data accounted for less than few percent of the total area and the values does not seem to be outliers they were considered here. Error bars are based on the rate of false alarms and misses according to the errors in Mazur and others (2017).

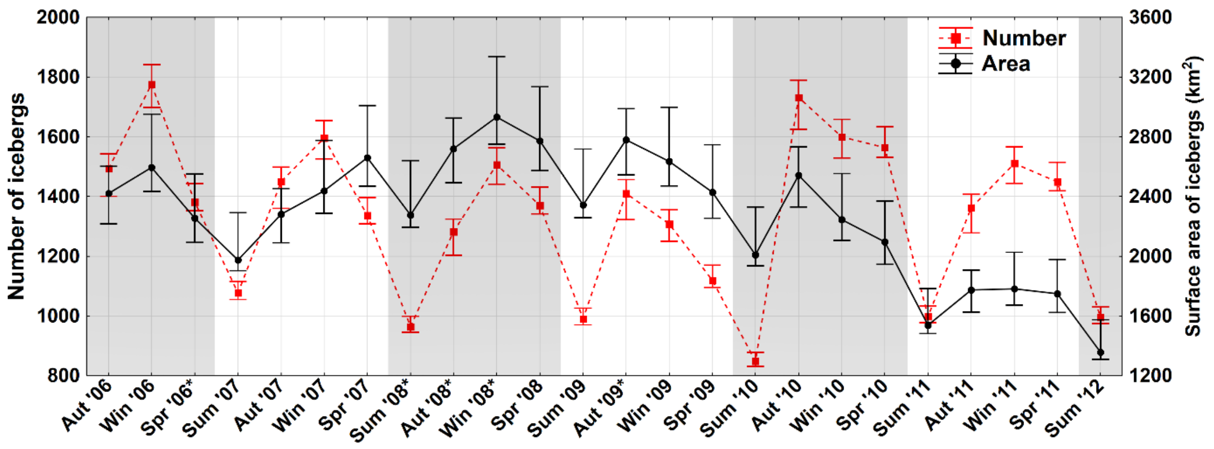

Figure 2. Seasonal averages of icebergs and associated surface area in the ASE: summer (Dec–Feb), autumn (Mar–May), winter (June–Aug), spring (Sep–Nov) between 2006-2012. Gray rectangles separate years according to seasons. Error bars represent the possible rate of false alarms and misses according to Mazur and others (2017). Incomplete data coverage is found in the seasons marked with an asterisk.

Clear seasonal periodicity is found in the time series, with typically larger numbers and surface area of icebergs experienced in the autumn, winter and spring months. This can be also seen in the seasonal cycle of icebergs characteristics in the ASE during the study period (Fig. 3).

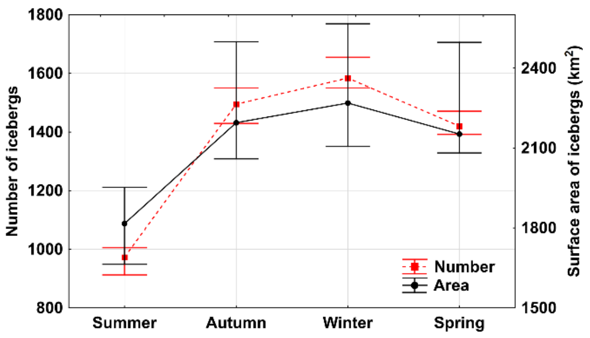

Figure 3. Seasonal cycle of icebergs and associated surface area in the ASE: summer (Dec–Feb), autumn (Mar–May), winter (June–Aug), spring (Sep–Nov) between 2006-2012. Error bars represent the possible rate of false alarms and misses according to Mazur and others (2017).

In Fig. 4, the average amount of icebergs in a 15 km × 15 km observation grid in different seasons between 1 January 2006 and 8 April 2012 is shown. It can be seen that not only the number of icebergs and their surface area change seasonally but the spatial distribution of icebergs in the basin changes in different seasons as well. In general, the average number of icebergs is quite constant in the ASE and the seasonal variation of the amount of icebergs in the ASE appears to be caused by variations in the area north of Pine Island Bay (Fig. 4), where mostly small icebergs (less than 2 km^2) are observed (Mazur and others, 2019).

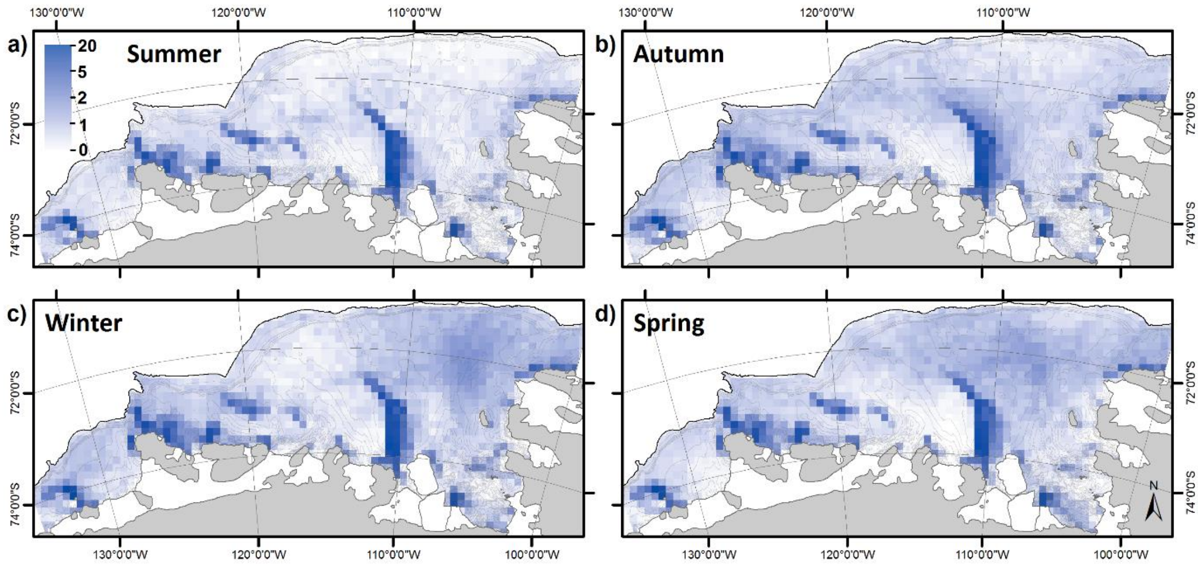

Figure 4. Average number of icebergs in a 15 m ×15 km observation grid in the ASE in different seasons: (a) summer (Dec–Feb), (b) autumn (Mar–May), (c) winter (June–Aug), (d) spring (Sep–Nov) between 1 Jan 2006–8 Apr 2012 (note that the color scale, depicting iceberg numbers, is non-linear in order to show low values clearly). The bathymetry is acquired from IBCSO database (Arndt and others, 2013).

4.2. Monthly changes of iceberg characteristics

We use the only two years of sufficient data coverage (2010-2011) to depict the monthly calving rates (Fig. 5). As can be seen, calving was the highest in late spring, summer and early autumn.

The contribution of individual ice shelves to the total calving is presented in Fig. 6, showing that except one large calving event from Western Getz and Thwaites in October 2011 the calving rate was lower in 2011 than in 2010. In 2010, the largest ice mass loss was observed in the first months of the year, and in 2011 it took place in winter and spring.

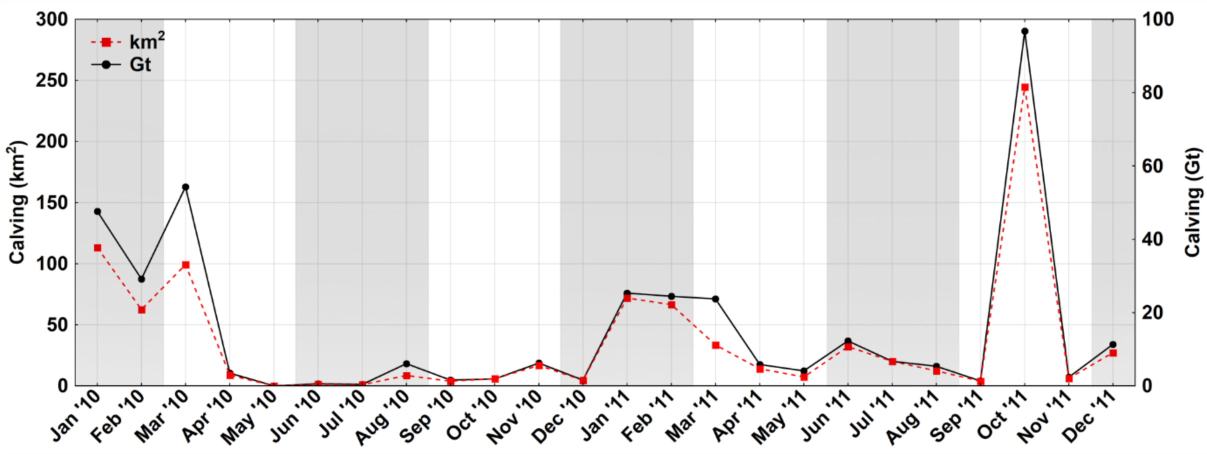

Figure 5. Monthly iceberg calving rates, in km^2 and in Giga tons, for the ASE between Jan 2010–Dec 2011. Gray rectangles separate the austral seasons: summer (Dec – Feb), autumn (Mar – May), winter (June – Aug), spring (Sep – Nov).

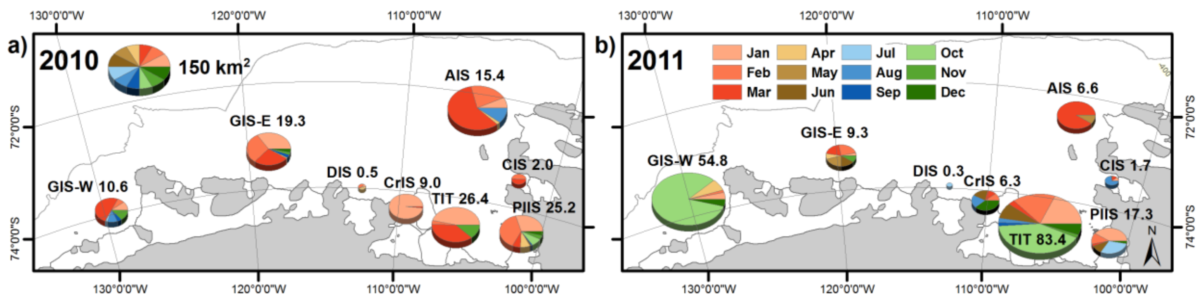

Figure 6. Iceberg calving rates at the various ice shelves in the ASE during (a) 2010 and (b) 2011. The pie charts show the average annual calving from the indicated ice shelves in km^2. The numbers depict the values in Gt. Ice-shelf names: AIS – Abbot Ice Shelf, CIS – Cosgrove Ice Shelf, PIIS – Pine Island Ice Shelf, TIT – Thwaites Ice Tongue, CrIS – Crosson Ice Shelf, DIS – Dotson Ice Shelf, GIS-E – Getz Ice Shelf East, GIS-W – Getz Ice Shelf West.

Fig. 7 shows monthly averages of number and surface area of icebergs in the ASE in 2010 and 2011. While the average number of icebergs does not vary significantly between 2010 and 2011, the surface area is significantly larger in 2010. In both years, both parameters show a minimum in austral summer, with an increase in January–March and a decrease in November–December. In 2010, there were two maxima, one in April/May and the other in August/September, while in 2011 there was only a single maximum during austral winter (peaking in September). The temporal variability has a similar pattern for both the amount and surface area of the icebergs.

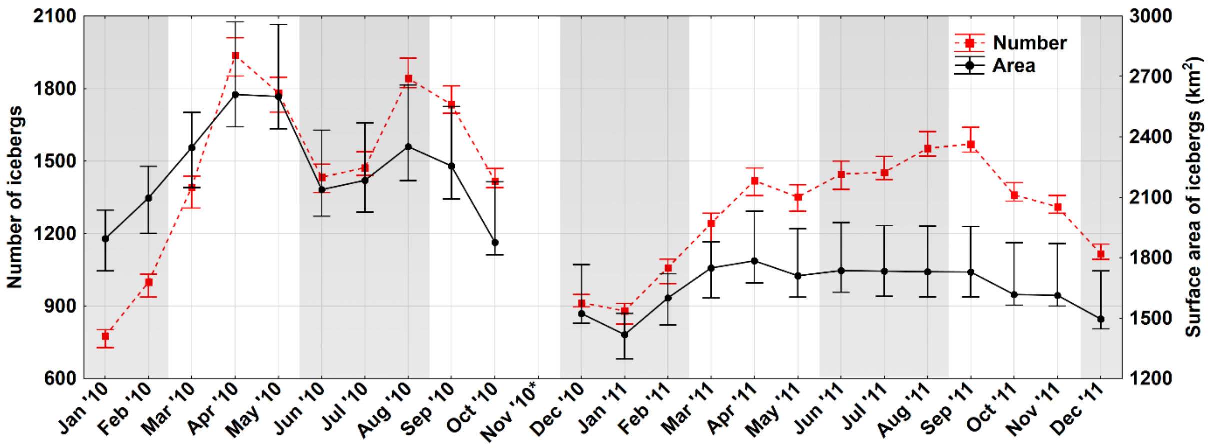

Figure 7. Monthly average total number of icebergs and their surface area in the ASE during 2010 and 2011. Gray rectangles separate Antarctic seasons: summer (Dec-Feb), autumn (Mar-May), winter (June-Aug), spring (Sep-Nov). Error bars represent the rate of false alarms and misses based on the classification results presented in Mazur and others (2017).

In order to study monthly spatial changes in iceberg distribution, Figs. 8 and 9 were constructed. The maps show the distribution anomaly (i.e., the monthly average values minus the annual average) for each grid cell. As already noted in Fig. 4, Pine Island Bay and the northern part of the shelf have the most dramatic changes (Figs. 8 and 9). However, a significant increase of iceberg number was also observed on the western part of the ASE in April and May of 2010. In both years, icebergs are moving into the north-eastern part during fall and are accumulating there throughout winter. When spring arrives, and sea ice thawing initiates, they begin to move again and drift into the western part of the ASE.

The example iceberg trajectories indicate that some portion of icebergs in the ASE originate from the Bellingshausen Sea. Also the circulation of an armada of icebergs can be seen in the north eastern area during the winter months, which is more spatially dispersed in 2010 than in 2011, with icebergs reaching more southerly locations during 2010. There is also a summertime migration of icebergs from the shallow ridge separating Pine Island Bay and Dotson trough.

In order to assess the environmental conditions that potentially impact the movement and distribution of iceberg in the ASE, we investigate the monthly state of sea ice concentration and ocean stress (calculated as a combination of wind- and sea ice-induced stress according to Kim and others, 2017) (Figs. 10 and 11). Lower sea ice concentration leads to higher surface stress values as expected, and the sea ice concentration is significantly lower in 2010 than in 2011. Additionally, in both years a clockwise circulation of the iceberg pack in the eastern part of the ASE is observed.

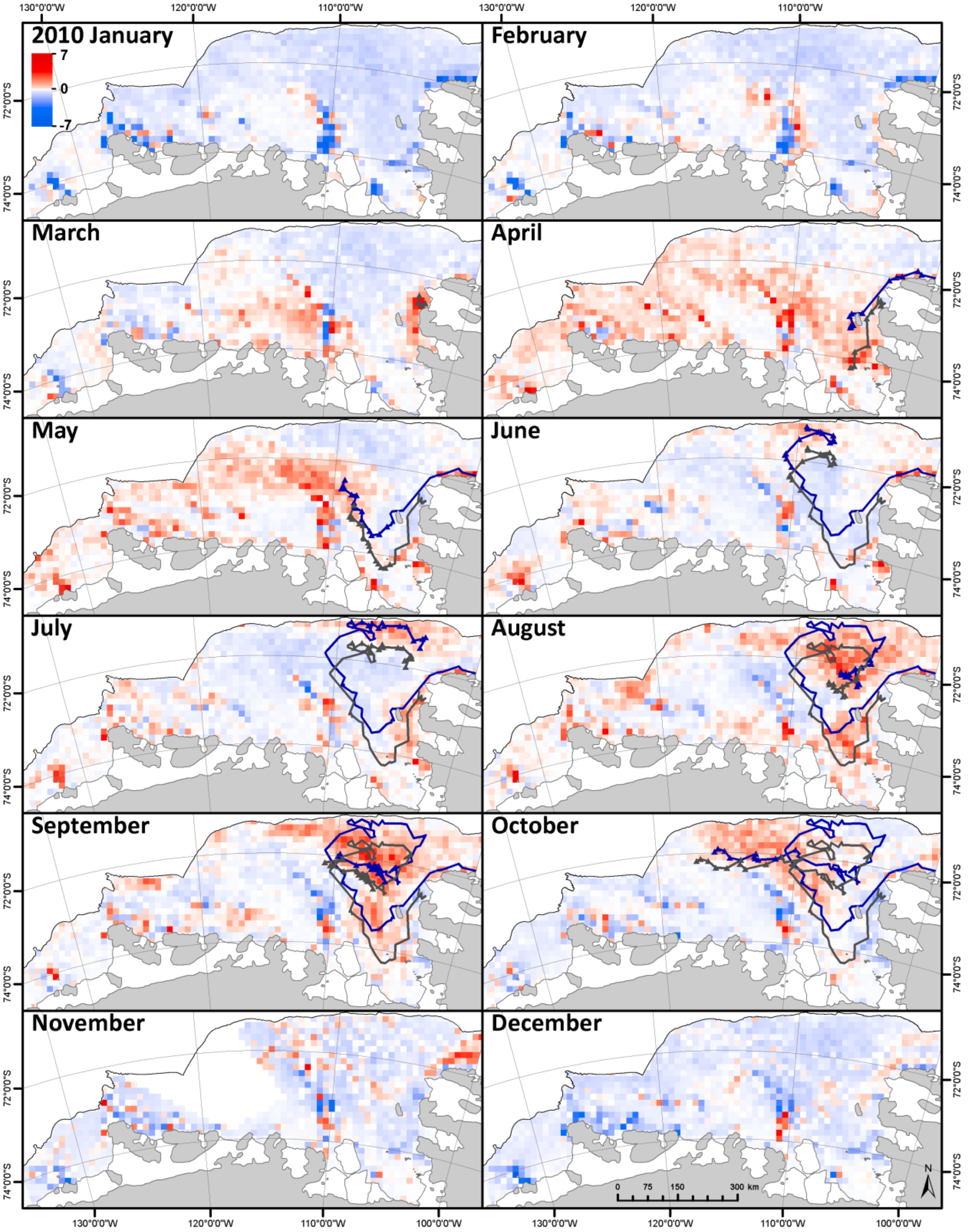

Figure 8. Difference between icebergs number in each particular month and the yearly average in a 15 km × 15 km observation grid in 2010. Lines represent a sample of iceberg trajectories with triangles as positions in a particular month.

273 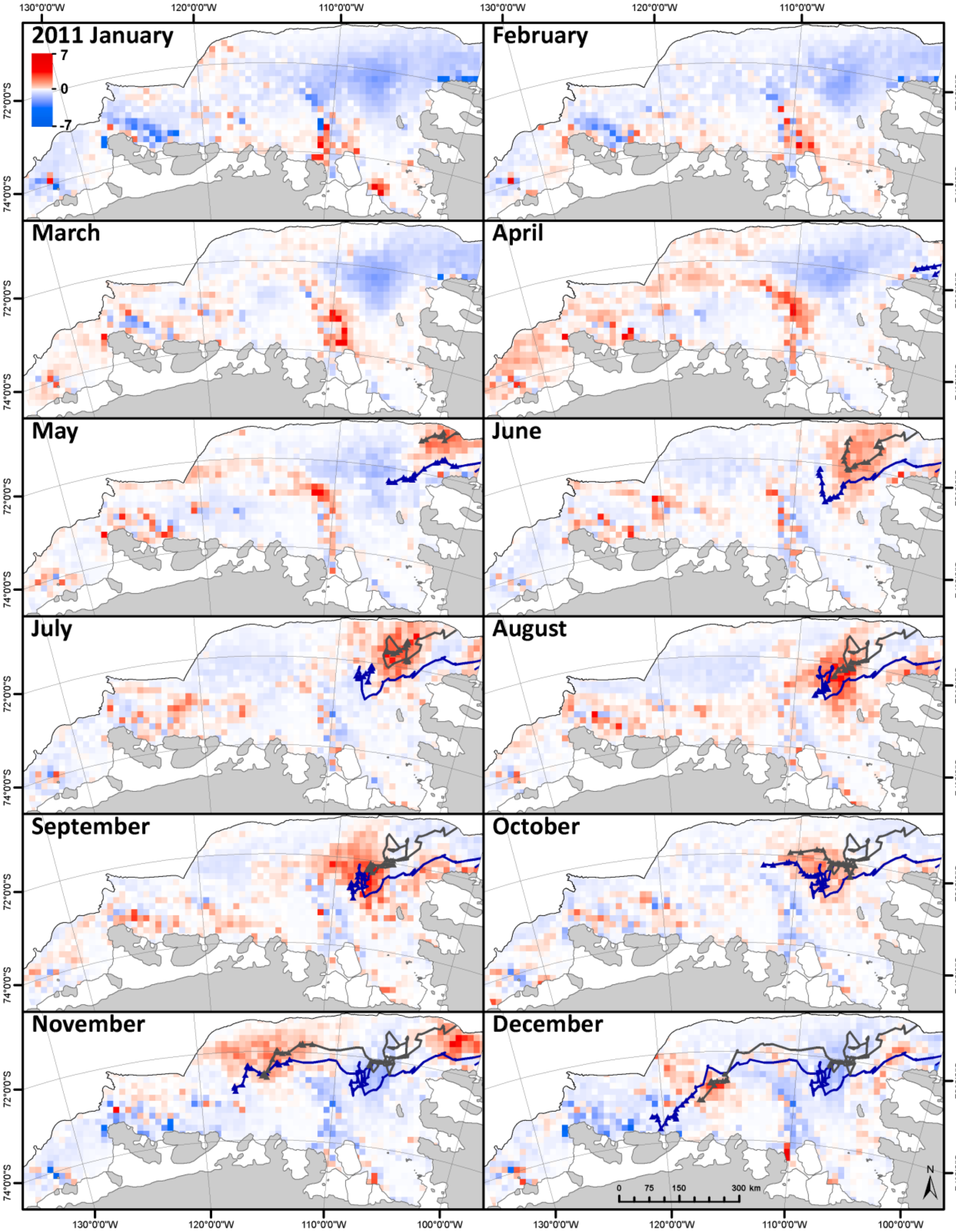

274 Figure 9. Same as Figure 8 but for 2011.

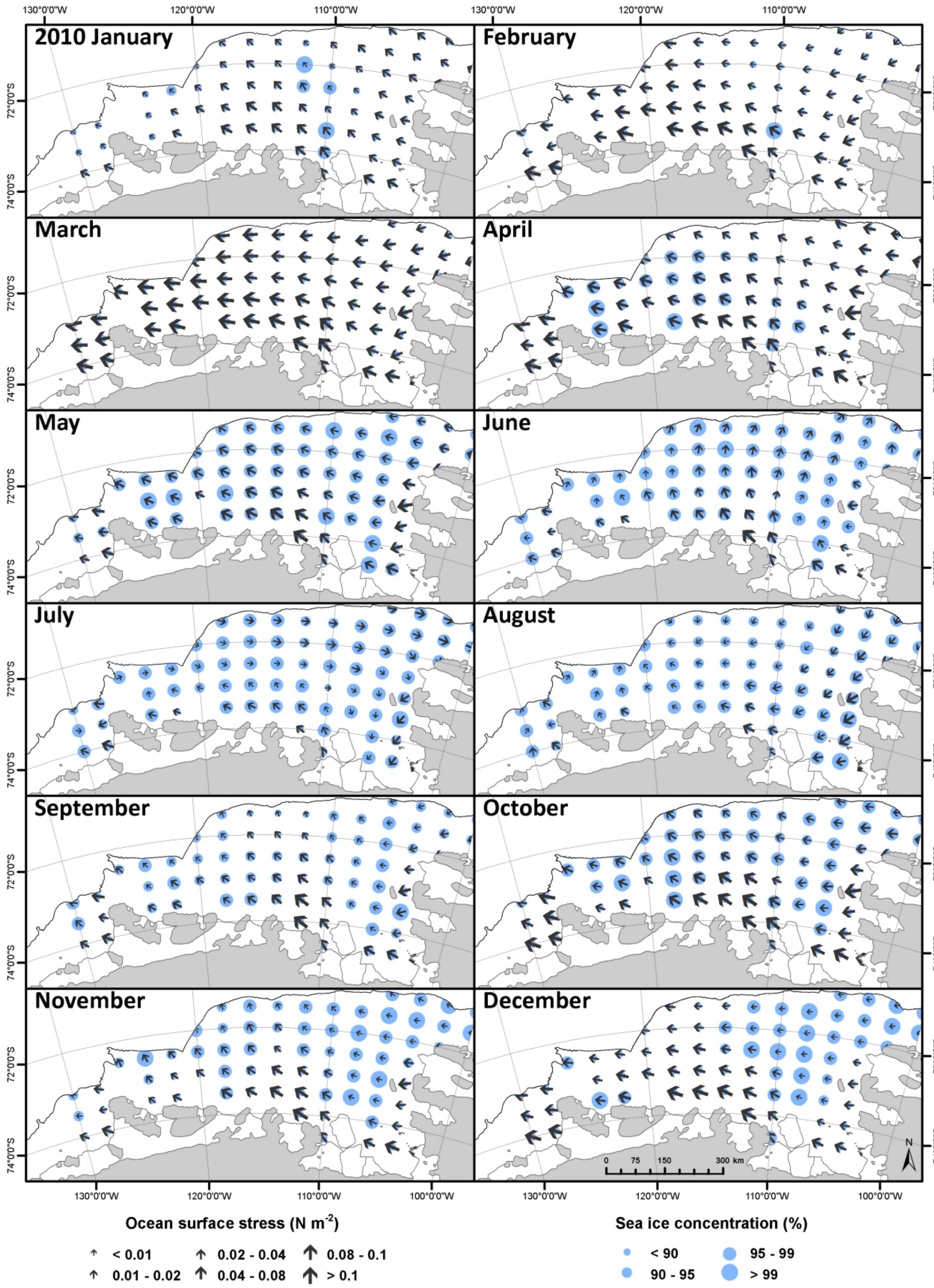

Figure 10. Monthly mean sea ice concentration from AMSR-E (Spreen and others, 2008) and ocean surface stress (Kim and others, 2017) in the ASE in the different months of 2010.

278

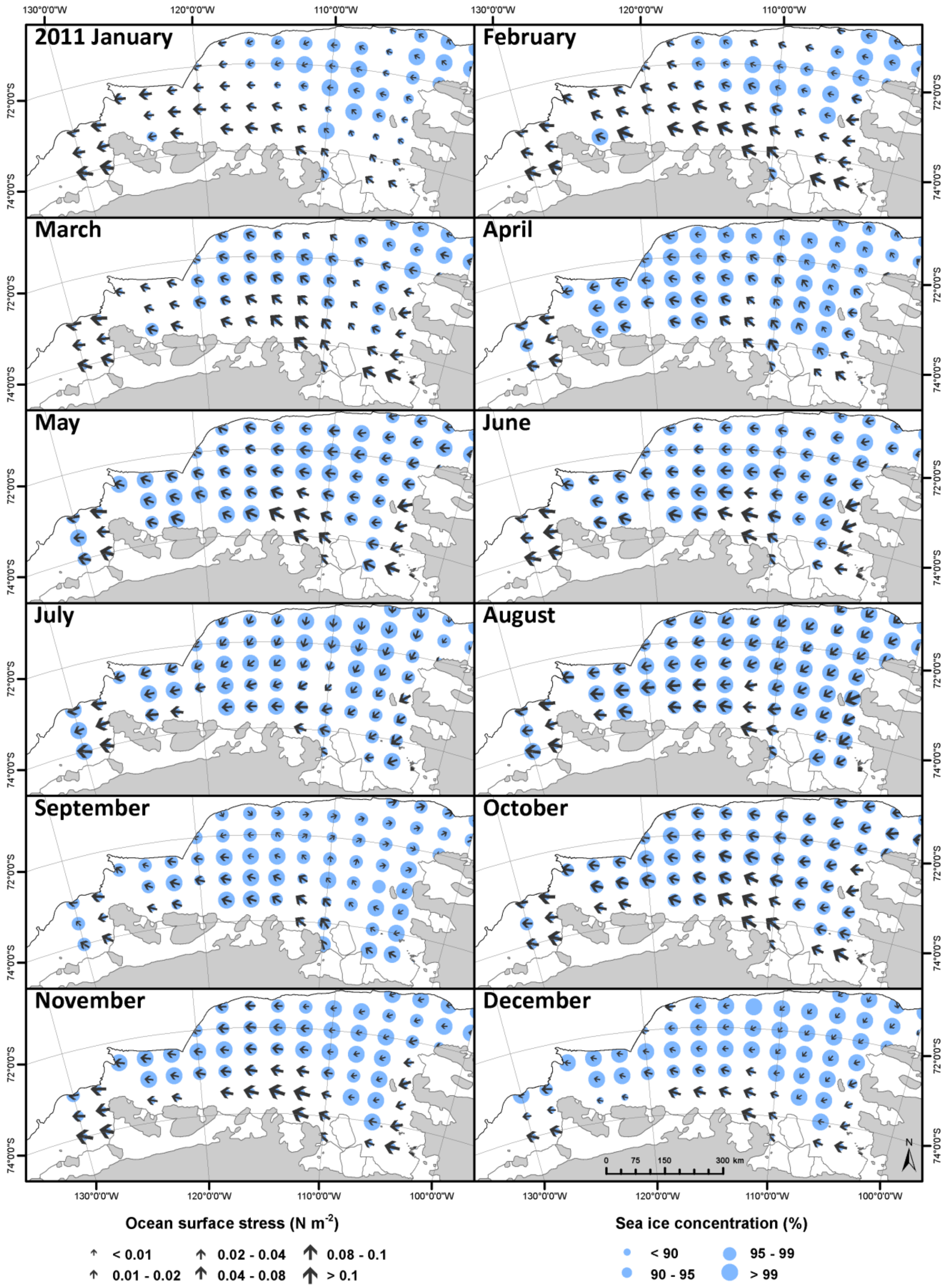
2011 January
February
March
April
May
June
July
August
September
October
November
December
130°0'0"W
120°0'0"W
110°0'0"W
100°0'0"W
72°0'0"S
74°0'0"S
0
75
150
300 km
N
Ocean surface stress (N m-2)
< 0.01
0.01 - 0.02
0.02 - 0.04
0.04 - 0.08
0.08 - 0.1
> 0.1
Sea ice concentration (%)
< 90
90 - 95
95 - 99
> 99

Figure 11. Monthly mean sea ice concentration from AMSR-E (Jan – Sep) and SSMIS (Oct – Dec) (Spreen and others, 2008) and ocean surface stress (Kim and others, 2017) in the ASE in the different months of 2011.

5. DISCUSSION

5.1 Seasonality and origin of icebergs

We observe a clear seasonal cycle in the near-coastal amount and surface area of icebergs, with a maximum during austral winter and minimum during austral summer (Figs. 2 and 3). The open-water results of Tournadre and others (2015) and Tournadre and others (2012) also show a seasonal variation of the amount of icebergs but with the maximum of amount of icebergs observed in summer. Thus our result is the opposite of what was expected, also considering that most of iceberg calving is also observed in austral summer (Fig. 5). However, the results of Tournadre and others (2015) and Tournadre and others (2012) pertain to open water only, i.e., a significantly smaller study area during winter than summer. Some coastal regions are never ice free and a large portion of icebergs are trapped in sea ice in coastal regions during the whole year, which indicates that the open-water results of Tournadre and others (2015) are not representative for the region considered and likely for many other Antarctic sea embayments (e.g., the Bellingshausen Sea or Ross Sea). According to Young and others (1998) the probability of finding icebergs is the highest near to the coast and decreases with distance away from the coast, which is confirmed by work of Wesche and Dierking (2015), who show that significant amounts of icebergs are present in the near-coastal area. Jacka and Giles (2007) also observed a significant interannual variation of iceberg concentration, particularly in the proximity of large ice shelves, pointing to an episodic nature of the calving phenomena. The above mentioned studies show that a high number of icebergs can be seen close to the coast during the whole year, indicating that the observation of seasonal variation in Tournadre and others (2015) is not appropriate when considering the entire Antarctic domain where icebergs occur.

Here the highest changes in iceberg distribution are observed in the area north of the Pine Island Bay (Fig. 4) where mostly icebergs smaller than 2 km^2 dominate the counts and surface area (Mazur and others, 2019). According to Gladstone and others (2001) and Rackow and others (2015) who modeled iceberg trajectories in the Southern Ocean, general westward drift of the icebergs is expected in the ASE. The changes observed in the northern part of the ASE may indicate processes that have not been fully understood before in the ASE and that are caused by not only locally calved icebergs but also icebergs drifting into the ASE from external sources. One potential source could be the Bellingshausen Sea.

Fig. 6 shows that most of the ice mass in the ASE is lost from Pine Island, Thwaites and Getz Ice Shelves, which is in agreement with Depoorter and others (2013), Rignot and others (2013) and Liu and others (2015) and calving events predominantly occur in summer and early autumn (Fig. 5). Fig. 5 and 7 show that the increase in the amount of icebergs and their surface area coincides with the time of most calving (summer and early spring). The minimum amount and surface area of icebergs observed in this study is in January. Considering that the mean drift velocities are quite high in the ASE in austral spring (Mazur and others, 2019) the majority of the mobile bergs present in the basin during the winter season could have already drifted outside of the ASE. It has to be mentioned here that melting and fragmentation of icebergs into pieces too small to be detected with the current resolution of SAR data can also decrease the number of icebergs in summer months. Nevertheless, the growth of both parameters is observed in January – April, which is mostly due to the high calving rates during those months (Fig. 5). Assuming that the calving in the Bellingshausen Sea in similar to the ASE occuring in late spring and summer (in fact might be earlier due to the shorter sea ice season as in Stammerjohn and others, 2015) and that the icebergs velocities are comparable to the ones obtained in the study region, icebergs formed in the Bellingshausen Sea can be expected in the ASE in late summer and early autumn. These icebergs together with those presumably calved in the ASE get frozen into the sea ice during winter, until the sea ice begins to melt allowing the icebergs to moves westwards once again in spring. These mobile icebergs usually remain present in the ASE for approximately a year (Mazur and others, 2019). However, to better understand these processes at higher temporal resolution, changes of iceberg calving and iceberg characteristics needed to be studied further.

In this study, monthly average distributions of icebergs and the example trajectories between 1 January 2010 and 31 December 2012 have been presented (Figs. 8 and 9). They indicate that the small icebergs, dominating the northern part of the shelf region, are imported from outside the ASE. The latest studies by Liu and others (2015) show that the ice mass loss due to iceberg calving in the Bellingshausen Sea is relatively high compared to other parts of Antarctica (74.5 Gt yr^{-1}, which corresponds to the surface area of 794.4 km^2). Other studies do not indicate such high calving rates where, for example, Rignot and others (2013) estimated the calving flux to be approximately 35 Gt yr^{-1} and Depoorter and others (2013) obtained 41 Gt yr^{-1}, while Liu and others (2015) included the disintegration of the Wilkins Ice shelf in the Bellingshausen Sea during 2009. Only in April 2009 was an area of 700 km^2 of glacial ice broken off Wilkins Sound. Thus, it is likely that the larger number of icebergs were imported into the ASE from the Bellingshausen Sea.

5.2 Drivers of iceberg motion and distribution in the ASE

Winter time observations show that icebergs are not entirely motionless in the north-eastern part of the ASE, but have a clockwise circulation that is likely conserved as a merged iceberg–sea ice pack during the winter season. This appears to be associated with groups of smaller icebergs, e.g., the movement of red patches (Figs. 8 and 9) drifting and moving with the surface shown by arrows and sea ice concentration indicated by blue circles (Figs. 10 and 11). Two iceberg trajectories in each year are shown in Figs. 8 and 9 as gray and blue lines illustrating this. In 2010, when the sea ice concentration was comparatively low in concentration, the icebergs were distributed more widely, compared to 2011. Furthermore, in 2010 the icebergs seemed to exit the ASE westward during June and July (which causes the reduction in surface area and number of icebergs seen in Fig. 7). Part of this pack seems to have been pushed into the ASE again in August 2010. The modelling results of Gladstone and others (2001) do not indicate a seasonal cycle in iceberg distribution, despite using seasonally varying wind forcing. The results presented here might reveal prominent local winter circulation patterns in the ASE, which are not present in global atmospheric reanalysis models used in the studies of Gladstone and others (2001). Our results (Figs. 8 and 9) also suggest that a similar pattern might be observed in the Bellingshausen Sea and that icebergs calved off the easternmost ice shelves drifted into the ASE in November 2011 together with the winter sea ice pack. This input seems to be higher in 2011 than in 2010, which might explain why the drop in iceberg numbers and their surface area is not as significant in 2011, as in 2010 (Fig. 7).

The surface area lost from ice shelves in the ASE (Fig. 5) corresponds to only about 70% of the increase of the area of icebergs (Fig. 7). The surface area loss from ice shelves in the ASE between January–April, when the highest growth in icebergs number and their surface area was observed, was 403.5 km^2 and 238.0 km^2 in 2010 and 2011, respectively. Most of the calving occurs in the eastern part of the basin and the iceberg speeds are relatively low during summer, indicating that only a small portion of the bergs leave the ASE between January–April. This suggests that autochthonous (formed locally) icebergs could contribute to the total growth in 65% and 75% in 2010 and 2011, respectively, and that allochthonous (of external origin) icebergs might account for about 25 – 35% of the total surface area of mobile icebergs in the ASE. Albeit these being assumptions, it shows that to fully understand the changes in the iceberg population and distribution in the ASE, further studies should be carried out in the Bellingshausen Sea.

Assuming that all the icebergs formed in the ASE between 2010 and 2011 are mobile and usually last in the basin about a year, and that the contribution from the Bellingshausen Sea is about 30% of the total surface area calved in the ASE between January–April, provides an average iceberg surface area flux of 655 km^2 yr^{-1}, which equates to a mass flux through the boundaries of the ASE of 135 Gt yr^{-1}. This assumes an average thickness of 250 m (Gladstone and others, 2001, Silva and others, 2006, Tournadre and others, 2012) and an average density of 822 kg m^{-3} (Wesche and Dierking 2015). The assumption that there are no stranded icebergs means that the upper bound of iceberg flux estimation is provided, however this is partially counterbalanced by the fact that grounded icebergs do become afloat eventually. Also a second inflow of icebergs from the Bellingshausen Sea is observed in November (Figs. 8 and 9). Nevertheless, this suggests that even up to 181 Gt ice mass in the ASE might be stored in icebergs which are grounded there (assuming the total average iceberg ice mass 316 Gt, Mazur and others, 2019). It has to be elucidated here that the average iceberg mass is calculated based on the data from the whole study period and the flux is calculated based on two year observations. Thus, the value of ice mass stored in the grounded bergs in the area remains an estimation. We currently lack the required data by which to provide a more precise estimate, which would be similar calculations of iceberg number and surface area changes in the Bellingshausen Sea.

Studies of Merino and others (2016) and Rackow and others (2017) show that there is seasonality in melt water distribution in the Southern Ocean and the highest values are observed in January and February, which is particularly evident in the Ross Sea and in the ASE (Merino and others, 2016). This is in contrary to the total number of icebergs observed here: The lowest number of icebergs was observed in the ASE in austral summer. One explanation can be that the assumption of the constant in time iceberg production implemented in the model of Merino and others (2016) is not likely to be true in the ASE (Fig. 8 and 9). On the other hand, the results of the model presented by Rackow and others (2017), with a set of observed iceberg positions, also show similar seasonality in melt water injection from icebergs as Merino and others (2016). However, in the model of Rackow and others (2017) not only small icebergs were taken into account. They noticed that if larger icebergs are included into the model the seasonality becomes less significant, which is likely due to increasing importance of basal melt, while wave erosion is less relevant.

In general, until icebergs remain in cold water or are frozen into sea ice, the melting of the submerged surfaces and wave erosion are negligible. This study suggests that the majority of icebergs in the ASE are observed during the winter season. Additionally, most of those icebergs are small, with the draft smaller than the depth of the thermocline. It is likely that even if the number of icebergs is quite high in winter in the ASE they do not contribute significantly to the melt water flux in that season. However, most significant changes in iceberg distribution are observed in the outer part of the shelf (Fig. 8 and 9). When the iceberg pack starts drifting again in austral spring, the importance of surface melt and wave erosion is expected to increase for the smaller icebergs.

6. CONCLUSIONS

There is a clear seasonal cycle in iceberg population and surface area in the ASE. The highest values of both parameters are observed during austral winter; the lowest, during austral summer. The changes concern mostly the icebergs smaller than 1 km^2 and pertain to the area north of the Pine Island Bay. This is a new result not previously studied in the literature.

A general westward drift of icebergs was observed in the ASE shelf area. The drift patterns and the seasonal variation of the distribution indicate that the drift of icebergs in the northern part of the ASE is strongly modulated by sea ice. In summer, there is little sea ice and the small bergs drift freely westward. In autumn, icebergs which presumably were calved in the Bellingshausen Sea, drift into the ASE shelf region and get frozen into the sea ice during winter. When the sea ice breaks up in spring they start to move westward again.

There appears to be two main sources of icebergs in the ASE: autochthonous (locally calved) and allochthonous (of external origin). The monthly distributions and example trajectories in 2010 and 2011 indicate that the small icebergs dominating the northern part of the shelf region are imported from the Bellingshausen Sea and they represent about 25–35% of the total surface area of mobile icebergs in the ASE. The upper bound iceberg flux estimate obtained in the present study between 2010–2011 is 654.8 km^2 yr^{-1}, which equates to an ice mass flux of 135 Gt yr^{-1}. This suggests that up to 181 Gt of the ice mass in the area is stored in icebergs, which are grounded there.

Even though there is a large number of icebergs present in winter, these are not expected to contribute significantly to the melt water injection into the water column. Most of these icebergs are small (<20 km^2), with their draft occurring above the thermocline. Thus, the melting of the submerged surfaces and wave erosion are likely small.

Acknowledgements

This work was supported by the Polish National Science Centre research grant no. 2016/20/T/ST10/00498 (“Detection, characterization and effects of icebergs in the ASE, Antarctica”) and was also part of my research work at University of Gothenburg, thanks to a Swedish Institute scholarship. SS was funded by a Wallenberg Academy Fellowship (WAF 2015.0186). We want to also acknowledge, the Academic Computer Centre in Gdansk (CI TASK) for MATLAB license.

ASAR images were provided by European Space Agency for the Cat-1 project C1P.5417.

References

Arndt JE and 15 others (2013) The International Bathymetric Chart of the Southern Ocean (IBCSO) Version 1.0–A new bathymetric compilation covering circum-antarctic waters. *Geophys. Res. Let.,* **40**(12), 3111–3117 (doi: 10.1002/grl.5041)

Arneborg L, Wåhlin AK, Björk G, Liljebladh B and Orsi AH (2012) Persistent inflow of warm water onto the central Amundsen shelf. *Nat. Geosci.,* **5**(12), 876–880 (doi: 10.1038/ngeo1644)

Bamber JL, Riva REM, Vermeersen BLA and LeBrocq AM (2009) Reassessment of the Potential Sea-Level Rise from a Collapse of the West Antarctic Ice Sheet. *Science,* **324**(5929), 901–903 (doi: 10.1126/science.1169335)

Barnes DKA (2017) Iceberg killing fields limit huge potential for benthic blue carbon in Antarctic shallows. *Glob. Change Biol.,* **23**(7), 2649–2659 (doi: 10.1111/gcb.13523)

Biddle LC, Kaiser J, Heywood KJ, Thompson AF and Jenkins A (2015) Ocean glider observations of iceberg-enhanced biological production in the northwestern Weddell Sea. *Geophys. Res. Lett*., **42**(2), 459–465 (doi: 10.1002/2014GL062850)

Depoorter MA and 6 others (2013) Calving fluxes and basal melt rates of Antarctic ice shelves. *Nature,* **502**(7469), 89–92 (doi: 10.1038/nature12567)

ESA (2007) *Envisat ASAR Product Handbook 2.2.* Technical report, European Space Agency

Fretwell P and 59 others (2013) Bedmap2: improved ice bed, surface and thickness datasets for Antarctica. *Cryosphere,* **7**(1), 375–393 (doi: 10.5194/tc-7-375-2013)

Gladstone RM, Bigg GR and Nicholls KW (2001) Iceberg trajectory modeling and meltwater injection in the Southern Ocean. *J. Geophys. Res.,* **106**(C9), 19903–19915, (doi: 10.1029/2000JC000347)

Hunke AC and Ackley SF (2001) A numerical investigation of the 1997–1998 Ronne Polynya. *J. Geophys. Res.*, **106**(C10), 22373-22382 (doi: 10.1029/2000JC000640)

Jacka TH and Giles AB (2007) Antarctic iceberg distribution and dissolution from ship-based observations. *J. Glaciol.*, **53**(182), 341–356 (doi: 10.3189/002214307783258521)

Jacobs S and 6 others (2012) The Amundsen Sea and the Antarctic Ice Sheet. *Oceanography*, **25**(3), 154–163 (doi: 10.5670/oceanog.2012.90)

Kim T and 6 others (2017) Is Ekman pumping responsible for the seasonal variation of warm circumpolar deep water in the Amundsen Sea? *Cont. Shelf Res.*, **132**, 38–48, (doi: 10.1016/j.csr.2016.09.005)

Lancelot C and 6 others (2009) Spatial distribution of the iron supply to phytoplankton in the Southern Ocean: a model study. *Biogeosciences*, **6**(12), 2861–2878 (doi: 10.5194/bg-6-2861-2009)

Liu Y and 7 others (2015) Ocean-driven thinning enhances iceberg calving and retreat of Antarctic ice shelves. *Proc. Natl. Acad. Sci. USA*, **112**(11), 3263–3268 (doi: 10.1016/j.rse.2018.07.028)

Mazur AK, Wåhlin AK and Krężel A (2017) An object-based SAR image iceberg detection algorithm applied to the Amundsen Sea. *Remote Sens. Environ.*, **189**, 67–83 (doi: 10.1016/j.rse.2016.11.013)

Mazur AK, Wåhlin AK and Kalén O (2019) The life cycle of small- to medium-sized icebergs in the Amundsen Sea Embayment. *Polar Res.* (in press)

Merino N and 6 others (2016) Antarctic icebergs melt over the Southern Ocean: climatology and impact on sea ice. *Ocean Model.*, **104**, 99–110 (doi: 10.1016/j.ocemod.2016.05.001)

Rackow T, Wesche C, Timmermann R, Hellmer HH, Juricke S and Jung T (2017) A simulation of small to giant Antarctic iceberg evolution: Differential impact on climatology estimates. *J. Geophys. Res.*, **122**(4), 3170–3190 (doi: 10.1002/2016JC012513)

Raiswell R, Benning L, Tranter M, and Tulaczyk S (2008) Bioavailable iron in the Southern Ocean: the significance of the iceberg conveyor belt. *Geochem. Trans.*, **9**(1), 7 (doi: 10.1186/1467-4866-9-7)

Rignot E, Jacobs S, Mouginot J and Scheuchl B (2013). Ice-Shelf Melting Around Antarctica. *Science*, **341**(6143), 266–270 (doi: 10.1126/science.1235798)

Schloesser F, Friedrich T, Timmermann A, DeConto RM and Pollard D (2019) Antarctic iceberg impacts on future Southern Hemisphere climate. *Nat. Clim. Change*, (doi: 10.1038/s41558-019-0546-1)

Silva TAM, Bigg GR and Nicholls KW (2006) Contribution of giant icebergs to the Southern Ocean freshwater flux. *J. Geophys. Res.*, **111**, C03004 (doi: 10.1029/2004JC002843)

Smith KL and 7 others (2007) Free-drifting icebergs: Hot spots of chemical and biological enrichment in the Weddell Sea. *Science*, **317**, 478–483 (doi: 10.1126/science.1142834)

Spreen G, Kaleschke L and Heygster G (2008) Sea ice remote sensing using AMSR–89-GHz channels. *J. Geophys. Res.*, **113**, C02S03 (doi: 10.1029/2005JC003384)

Stammerjohn S. and 9 others (2015) Seasonal sea ice changes in the Amundsen Sea, Antarctica, over the period of 1979–2014. *Elementa–Sci. Antrop.*, **3**, 1–20 (doi: 10.12952/journal.elementa.000055)

Stern AA and 10 others (2015) Wind-driven upwelling around grounded tabular icebergs. *J. Geophys. Res.*, **120**(8), 5820–5835 (doi: 10.1002/2015JC010805)

Tournadre J, Bouhier N, Girard-Ardhuin F and Rémy F (2015) Antarctic icebergs distributions 1992–2014. *J. Geophys. Res.*, **121**(1), 327–349 (doi: 10.1002/2015JC011178)

Tournadre J, Girard-Ardhuin F and Legrésy B (2012) Antarctic icebergs distributions, 2002–2010. *J. Geophys. Res.*, **117**, C05004 (doi: 10.1029/2011JC007441)

Wesche C and Dierking W (2015) Near-coastal circum-Antarctic iceberg size distributions determined from Synthetic Aperture Radar images. *Remote Sens. Environ.*, 156, 561–569 (doi: 10.1016/j.rse.2014.10.025)

Wåhlin AK, Yuan X, Björk G and Nohr C (2010) Inflow of Warm Circumpolar Deep Water in the Central Amundsen Shelf. *J. Phys. Oceanogr.*, **40**(6), 1427–1434 (doi: 10.1175/2010JPO4431.1)

Young NW, Turner D, Hyland G and Williams RN (1998) Near-coastal iceberg distribution in East Antarctica, 50–145°E. *Ann. Glaciol.*, **27**(1), 69–74 (doi: 10.3189/1998AoG27-1-68-74)